The various states of von Willebrand factor and their function in physiology and pathophysiology

Volker Huck[1]; Matthias F. Schneider[2]; Christian Gorzelanny[1]; Stefan W. Schneider[1]

[1]Heidelberg University, Medical Faculty Mannheim, Department of Dermatology, Experimental Dermatology, Mannheim, Germany; [2]Boston University, Department of Mechanical Engineering, Boston, Massachusetts, USA

Summary

The specific interactions of von Willebrand factor (VWF) with the vessel wall, platelets or other interfaces strongly depend on (a shear-induced) VWF activation. Shear flow has been shown to induce a conformational transition of VWF, but is modulated by its thermodynamic state (state-function relationship). The state in turn is determined by physical (e.g. vessel geometry), physico-chemical (e.g. pH) and molecular-biological (e.g. mutants, binding) factors. Combining established results with recent insights, we reconstruct VWF biology and its state-function relationship from endothelial cell release to final degradation in the human vasculature. After VWF secretion, endothelial-anchored and shear activated VWF multimers can rapidly interact with surrounding colloids, typically with platelets. Simultaneously, this VWF activation enables ADAMTS13 to cleave VWF multimers thereby limiting VWF binding capacity. The subsequent cell-surface dissociation leads to a VWF recoiling to a globular conformation, shielding from further degradation by ADAMTS13. High local concentrations of these soluble VWF multimers, transported to the downstream vasculature, are capable for an immediate reactivation and re-polymerisation initiating colloid-binding or VWF-colloid aggregation at the site of inflamed endothelium, vessel injuries or pathological high-shear areas. Focusing on these functional steps in the lifecycle of VWF, its qualitative and quantitative deficiencies in the different VWD types will facilitate more precise diagnostics and reliable risk stratification for prophylactic therapies. The underlying biophysical principles are of general character, which broadens prospective studies on the physiological and pathophysiological impact of VWF and VWF-associated diseases and beares hope for a more universal understanding of an entire class of phenomena.

Keywords

VWF, shear stress, ADAMTS13, TTP, VWD

Correspondence to:
Prof. Dr. Stefan W. Schneider
Department of Dermatology, Experimental Dermatology
Heidelberg University, Medical Faculty Mannheim
Theodor-Kutzer-Ufer 1–3
68167 Mannheim, Germany
Tel: +49 621 383 6901, Fax:+49 621 383 6903
E-mail: stefan.schneider@medma.uni-heidelberg.de

or

Prof. Dr. Matthias F. Schneider
Biological Physics Group
Boston University, Department of Mechanical Engineering
110 Cummington Street
Boston, MA 02215, USA
Tel.: +1 617 353 3951, Fax: +1 617 353 3951
E-mail: mfs@bu.edu

Received: September 27, 2013
Accepted after major revision: February 8, 2014
Prepublished online: February 27, 2014

http://dx.doi.org/10.1160/TH13-09-0800
Thromb Haemost 2014; 111: 598–609

Introduction

The multimeric glycoprotein von Willebrand factor (VWF) is a well-known key player of primary haemostasis (1-9). Stored in intraendothelial Weibel-Palade bodies (WPB), VWF is co-localised with the proinflammatory proteins P-selectin, angiopoietin2, eotaxin3 and, among others, the cytokine interleukin (IL)-8 (10, 11). Upon stimulatory conditions, VWF as prerequisite for WPB genesis is released in company switching the endothelial cells (EC) from an antiinflammatory and anticoagulatory to a proinflammatory and procoagulatory surface (12-15). Thus, its role in inflammation and furthermore its impact on metastatic processes are matter of recent studies.

Mainly synthesised in ECs (and megacaryocytes for platelet VWF), VWF monomers underlie a specific post-translationally maturation process ending up in WPBs as assembled organised tubules of VWF multimers. Currently the total size of these VWF multimers remains unclear. However an estimate may be given based on the size of WPBs (2 μm length and 0.1 μm diameter) (9), the molecular weight (MW) of VWF (approx. 500 kDa of a dimer) and a typical protein density of roughly 1.3 g/cm^3 (16), which leads to approximately 10,000 to 50,000 dimers within one individual

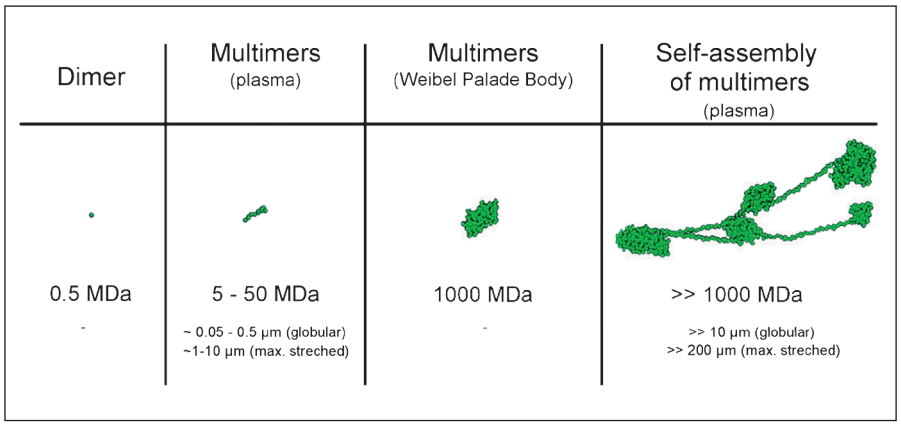

Figure 1: Molecular weight distributions of VWF. The molecular weight distribution of multimers in plasma reflects the current state of gel electrophoretical analysis. Molecular weight distribution of multimers in Weibel-Palade Bodies is a theoretical estimation based on the vesicle volume. The molecular weight of self-assembled multimers is impossible to measure experimentally; however, a size of more than several GDa could be expected. The indicated size ranges of globular and maximal stretched VWF multimers in plasma could be considered only as rough estimates.

WPB. This corresponds to a MW of more than 1 GDa, which is significantly above the size detectable in typical VWF gel analysis (17, 18). Although this seems immense, immunofluorescence images reveal sizes around several 100 µm (see ►Figure 5A), consistent with the MW of ~1 GDa (14, 19-21). Based on our earlier work (22, 23), we propose that this exceptionally large size of VWF constitutes the prerequisite to respond to hydrodynamic forces and their variations. ►Figure 1 summarises the molecular weight distributions of VWF.

Upon EC activation for instance by thrombin, histamine, vascular endothelial growth factor, fibrin, tumour necrosis factor alpha, reperfusion or tumour cells (10, 12, 24-26) VWF is released both into the subendothelial matrix and the blood flow, respectively (7, 27, 28). Subsequently exposed to the hydrodynamic forces of blood flow while remaining anchored to the endothelium, this freshly released ultra-large VWF (ULVWF) reversibly transforms from a globular to a stretched conformation and therefore exposes binding sites as well as its cleavage site in a shear-dependent manner (22, 23, 29, 30). Each VWF multimer subunit contains binding sites for platelet glycoprotein (GP) Iba, heparin, collagen, GPIIb/IIIa, factor VIII, ADAMTS13 and other ligands. In particular, over a wide range of shear rates VWF contributes to the fully reversible arrest even of inactivated platelets (31) and thrombus formation by interaction of its exposed A1 domain with GPIba with putative selectine-like kinetics. However, in contrast to platelet bonds of other molecules due to the biomechanical properties of receptor-ligand bindings, the VWF A1 domain-GPIba interaction was shown to be the only sufficient source to initiate platelet adhesion under high shear conditions (32). It should be noted that there is a discrepancy between this threshold in human and mouse blood of a factor of approx. 4 (500 to 800 s^{-1} in human blood versus 2,000 to 5,000 s^{-1} in mouse blood) (33-35). Considering the complex physiological situation involving not only the isolated shear dependency of VWF but also the influence of shear flow conditions on platelet shape conformation (36), on VWF-GPIba interactions (37) and on VWF-surface adsorption (38, 39), we aim to mainly focus on the conformational activation of VWF and its physiological relevance.

The metalloproteinase ADAMTS13 was shown to be the specific plasma protease regulating the length and binding capacity of VWF fibres in the human vasculature, constantly cleaving VWF multimers at the A2 domain cleavage site (40). Causing the appearance of smaller VWF fragments in normal plasma, the cleavage of VWF fibres first leads to a detachment from the endothelium and the further degradation to its loss of shear-dependent binding function. Hence, degradation of VWF by ADAMTS13 is highly enhanced under high shear flow conditions and in the case of elongated/stretched VWF multimers presumably due to an increased accessibility of the cleavage site within the A2 domain (21, 23).

Focusing on the new insights in VWF's state-function relationship under various shear regimens, this manuscript gives an update of state-of-the-art and novel *in vitro* techniques, their application in a broadened field of pathophysiological interest and their clinical implications for VWF associated diseases.

Short overview of VWF associated diseases

The investigation of different subtypes of hereditary mutations of VWF in von Willebrand disease (VWD), the acquired von Willebrand syndrome (AVWS) and cleavage enzyme defects in thrombotic thrombocytopenic purpura (TTP) on both molecular and individual patient's level have a beneficial scientific effect from bench to bedside and vice versa and therefore help to understand the underlying mechanistic backgrounds for VWF function.

von Willebrand disease (VWD)

VWD is the most common hereditary bleeding disorder caused by a deficiency or dysfunction of VWF. Three types of VWD are classified: VWD type 1 is a quantitative defect characterised by depressed levels of VWF with regular functionality. The second quantitative variation is the severe bleeding disorder VWD type 3 with an almost complete absence of VWF levels. In contrast, the classification VWD type 2 subsumes a wide variety of structural and/or functional defects of VWF due to mutations in distinct domains of the molecule affecting the process of multimerisation, the release, or the binding capacity to different interaction partners impairing platelet adhesion or factor VIII binding (41).

Dependent on the type of mutation, clinical symptoms range from mild diathesis to rare severe episodes of mucosal bleedings and intraarticular or intramuscular bleeding. Adequate medical attendance is necessary for prophylaxis or treatment of bleeding episodes. The most important therapeutic regimens target to boost functional active VWF plasma levels to haemostatically active concentrations comprising enforced stimulation of WPB exocytosis using the antidiuretic hormone analogon 1-desamino-8-D-arginine vasopressin (DDAVP) or VWF replacement therapy by infusion of plasma-derived VWF containing concentrates (18, 41).

Acquired von Willebrand syndrome (AVWS)

The bleeding disorder AVWS is an often misdiagnosed syndrome characterised by non-inherited secondary structural and/or functional defects of VWF due to an increased proteolysis under exceeding shear flow conditions, an increased antibody-mediated clearance or an augmented adsorption to malignantly transformed cell surfaces (42, 43). Regularly, a causative therapy will also cure the haemorrhagic diathesis. For prophylaxis or acute bleeding episodes a VWF replacement therapy (comparable to the treatment of VWD) or intravenous infusion of immunoglobulin G is recommended. For DDAVP treatment, the response rate to achieve a significant plasmatic VWF concentration depends on the various underlying diseases; e.g. it is high beneficial for neoplasm-induced AVWS but of low potency for antibody-mediated AVWS (44).

Thrombotic thrombocytopenic purpura

The haematological disorder thrombotic thrombocytopenic purpura (TTP) is a secondary VWF-associated disease. There are two types of this disease, the Moschcowitz syndrome as acquired TTP with reduced activity of ADAMTS13 due to autoantibodies and the Upshaw-Schulman syndrome with an inherited deficiency of ADAMTS13 (45). Affecting the specific cleavage enzyme of VWF, unusually large VWF multimers with a higher platelet binding capacity have been systemically detected in the plasma of patients suffering from TTP (46). Here it may be hypothesised that the above calculated size of several 100 µm of freshly released VWF may persist without further degradation and is capable to unleash an unforeseen potency for platelet binding. Therefore, TTP is associated with life-threatening depositions of platelet-ULVWF thrombi in the microvasculature leading to platelet consumption followed by thrombocytopenia and bleeding episodes (45, 47). Moreover, interfering in the functional homoeostasis of VWF release and subsequent cleavage, it was shown that IL-6, thrombin and reactive oxygen species, all elevated under inflammatory conditions, further dampen ADAMTS13 activity (48-50). The therapeutic options in acquired TTP include periodical plasma exchange therapy, immunosupressants and plasmapheresis. In the case of the congenital Upshaw-Schulman syndrome plasma substitution is the therapy of choice. In the near future, a supplementation with recombinant ADAMTS13 may be available.

For a comprehensive diagnostic characterisation of VWF-related diseases, patients and clinicians will benefit from the correlation of genetic tests, enzyme activity assays, VWF multimer analysis and the performance of new assays on the functional characteristics of VWF.

Functional states of VWF

Upon stimulated EC release of VWF multimers into the blood flow, the biopolymer meets at least two relevant changes in its surrounding milieu: a pH shift from an acidic to a physiological pH (51, 52) and the exposition to shear stress. During the process of exocytosis the densely packed and helically assembled VWF in the acidic WPBs underlies a spontaneous shift in pH starting from side of the fusion pore at the EC membrane (51, 53-55). This leads to an entanglement-free elongation of the multimer in the direction to the vessel lumen where it is exposed to the hydrodynamic force of the flowing blood. Still anchored at the EC surface via integrin alpha(v)beta (3, 56), P-selectin (57), lipid membranes (58) or WPBs, VWF becomes "activated" when going through a reversible globule-stretch transition to VWF fibres (23), therefore presumably providing a sufficient density of binding sites in the enrolled A1 domain for platelet adhesion. Simultaneously, the A2 domain experiences an increased exposure to interact with the VWF-cleaving enzyme ADAMTS13 (59). This parallel occurrence of shear-induced haemostatic activation and subsequent cleavage provides a self-regulatory mechanism avoiding excessive fibre formation under physiological conditions (19). These transitions of isolated VWF disregarding further interaction partners are depicted in ▶Figure 2, utilising images from computer simulations, illustrating schemes (▶Figure 2A) and experimental images taken by atomic force microscopy (▶Figure 2B) and immunofluorescence microscopy (▶Figure 2C), respectively.

VWF as a polymer under flow

From the biophysical point of view, the seemingly counterintuitive amplification in polymer adhesiveness by the increase of flow-induced shear stress becomes plausible: Although high shear flow is naturally accompanied by an increase of lift forces, this effect is overwhelmed by the subsequent transition of VWF baring numerous formerly shielded tensile binding regimes when changing its conformation. This fluid dynamics affected process is amplified as the shear rates increase up to 10,000 s^{-1} (36). We could previously show that a critical shear rate of 1,000 to 5,000 s^{-1} activates VWF under unbound (soluble) conditions. It seems likely that critical shear rates under bound or adsorbed conditions are somewhat lower (~200 s^{-1}) (19, 60) and will render VWF in a state of higher activity. These shear rates may be reduced by physical, physicochemical or biological factors, as for instance channel geometry, pH or mutations. This could explain that even in venules ADAMTS13 is crucial for the regulation of platelet adhesion and aggregation in histamine stimulated vessels (61). Since ADAMTS13 only cleaves activated VWF, it is very likely that activation can also take place in venules, where shear rates fall way

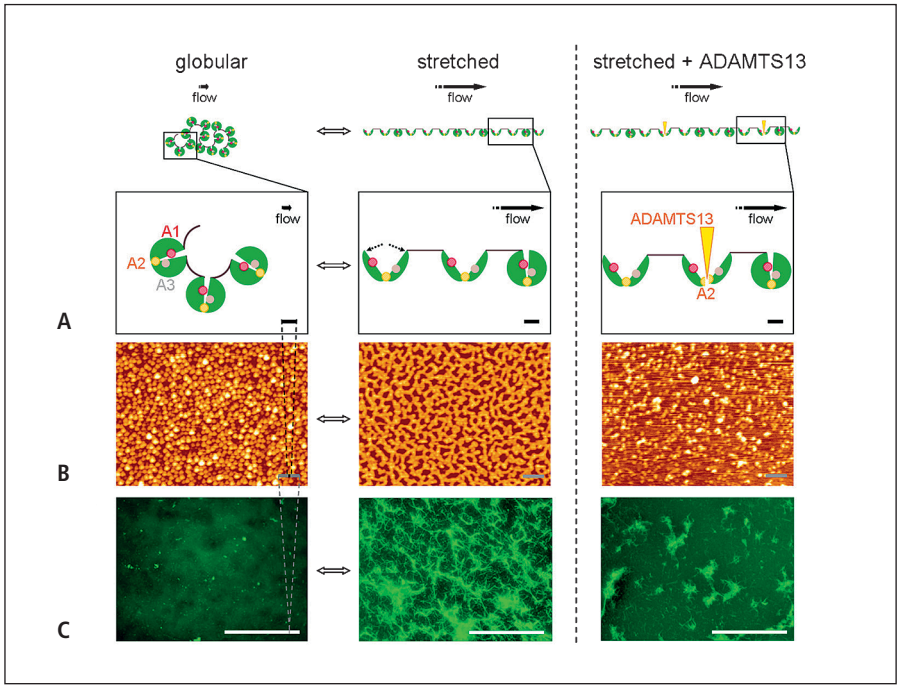

Figure 2: Shear-induced VWF activation and degradation from the monomer to the microscopic level. A) Illustrating scheme of a VWF fibre from globular to stretched transition under rising shear on the monomer (green circle) level. Under low-shear conditions, the A domains A1 (red) and A2 (yellow), are shielded (left). Above a critical shear rate, the VWF fibre reversibly enrols and the A domains become exposed (middle). In the presence of ADAMTS13, stretched VWF is degraded at the A2 domain (right). Scale bars correspond to 10 nm. B) Height-coded atomic force microscopic images of VWF transition. Monomers appear as yellow dots covering the surface (left). Under shear flow, VWF monomers / dimers polymerise to a structured two-dimensional network (middle). In the presence of ADAMTS13 this network is efficiently degraded (right). Scale bars correspond to 100 nm. C) Immunofluorescence images of VWF stained in green from the globular (left) to the stretched state (middle) in the absence or presence (right) of ADAMTS13. Scale bars correspond to 100 µm. Experiments based on our earlier work (21).

below 500 s^{-1}. Therefore, one can speculate that shear activated VWF potentially plays a significant role in the initiation of venous thrombosis as elegantly shown in a mouse model (62). As the local wall shear rate in the human microvasculature is determined to be in the order of 100 to 8,000 s^{-1} (63, 64), the process of VWF unfolding is in fact of relevance also under physiological conditions. At vessel injuries, vasoconstrictions or stenotic compartments the reduction of the vessel lumen can rise the shear rates to excessive levels above 50,000 s^{-1} (65) or induce elongational flow conditions (see below). Using smart *in vivo* as well as *in vitro* experiments, Nesbitt et al. could clearly show that shear microgradients, typically occurring at stenotic vessels control initial and reversible platelet recruitment at high shear zones (36). This interaction was exclusively VWF-GPIba mediated confirming the importance of a shear activation of VWF (66).

From a pure polymer perspective, a prerequisite for the globule-stretched transition behaviour is the "correct" size of the repeating units assembling the multimeric VWF and, presumably to a lesser extent, the length of the multimer (23). The functional active repeating unit consists of two disulfide-linked monomers (= dimer) with a collective molecular mass of ~500 kDa and a size of ~70 nm and ~10 nm along the long and the short axis, respectively (67). Scaling arguments (22), which include hydrodynamic interactions, reveal a very sensitive size dependence of the critical shear rate $\dot{\gamma}_{crit}$ for the globule-stretched transition

$$\dot{\gamma}_{crit} \sim \frac{1}{a^3},$$

where a should be seen as an effective size of a repeating unit. For instance, an increase in a by a factor of 10, is therefore expected to reduce the critical shear by a factor of 1,000. Considering the unusually large repeating units of VWF, it seems that VWF is the result of a Darwinian optimisation process for a protein that sensitively responds to shear stress in the regime of physiological flow.

Hydrodynamic stress can be applied on a protein in flow by at least two fundamentally different mechanisms: by shear stress as described and by elongational stress. Broadly speaking, the first is the result of a velocity gradient perpendicular to the wall while the second arises when the flow velocity changes in flow direction. In the latter, the end of the polymer experiences a different velocity than the front creating accelerating forces. Similar to the shear rate, a rate of elongation $\dot{\varepsilon}$ can be defined. In ▶Figure 3 this is well approximated by

$$\dot{\varepsilon} = \frac{\Delta v_z}{D} = \frac{v_1\left(\frac{r_1^2}{r_2^2} - 1\right)}{D},$$

where Δv_z is the change of velocity over the distance D in flow direction (z-direction) and r_1 and r_2 the radii before and after the constriction. Just like in shear flow, this creates tensile forces along the polymer. Interestingly, Sing and Alexander-Katz have found that elongational stresses are much more effective in the sense that – theoretically – an $\dot{\varepsilon}$ of 300 to 600 s^{-1} leads to polymer stretching while necessary shear rates $\dot{\gamma}$ have to be about one to two orders of magnitude larger for the same polymer model (68). The authors argue, that the significant platelet aggregation at stenotic conditions observed by Nesbitt et al. (36) appears to be a result of the strong elongational forces (69).

Hydrodynamics further tells us, that shear flow can be considered as a superposition of elongation and rotational flow. The only relevant contribution for polymers to be stretched is the

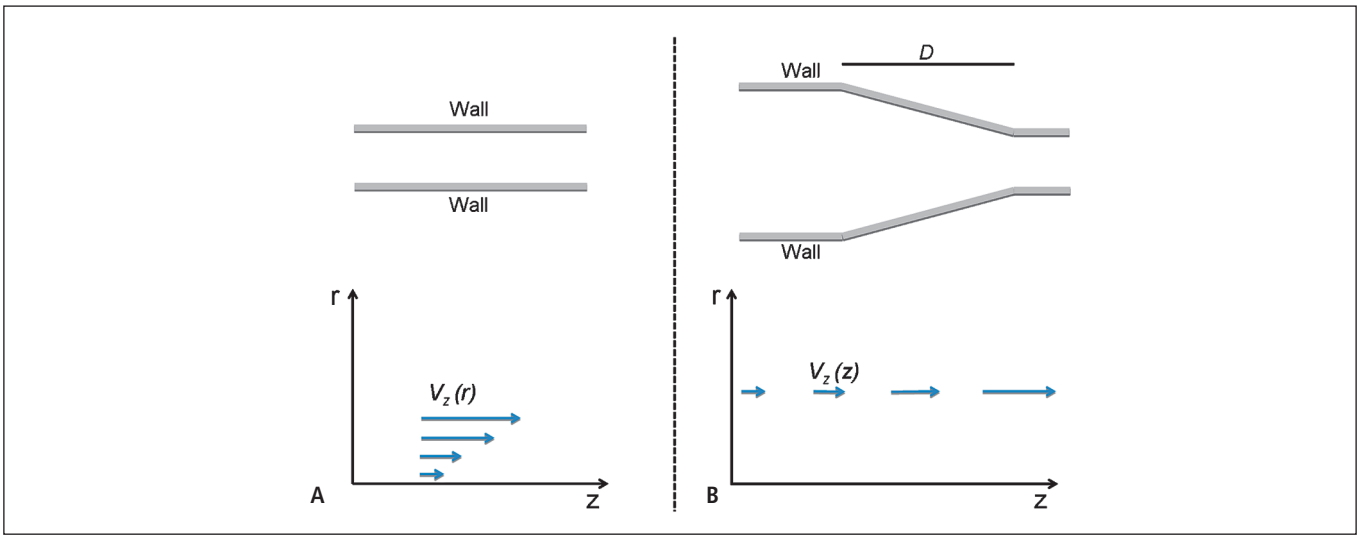

Figure 3: Shear and elongational flow. While the wall shear rate (A) is simply the rate of change of the velocity component V_z away from the wall (radial direction r), elongational flow (B) is characterised by the increase of V_z along z and predominately the result of geometrical variations of the vessel. Hence particular important at vasoconstriction or stenotic conditions (68).

strength of the elongation component. In other words, reducing the rotational component for the sake of an increase in elongational flow would likely facilitate VWF activation under otherwise identical conditions. Physiologically this is important for several reasons. First, whenever near an interface, the rotation of an object is reduced. VWF elongation is therefore expected to be facilitated at the vessel wall or nearby a blood platelet (22). Second, geometrical parameters, as for instance during stenotic conditions, may support a more "funnel-like" flow, which would increase the elongational flow in the centre of the funnel (recall, that in pure shear flow, the shear stress is exactly zero in the centre) (68).

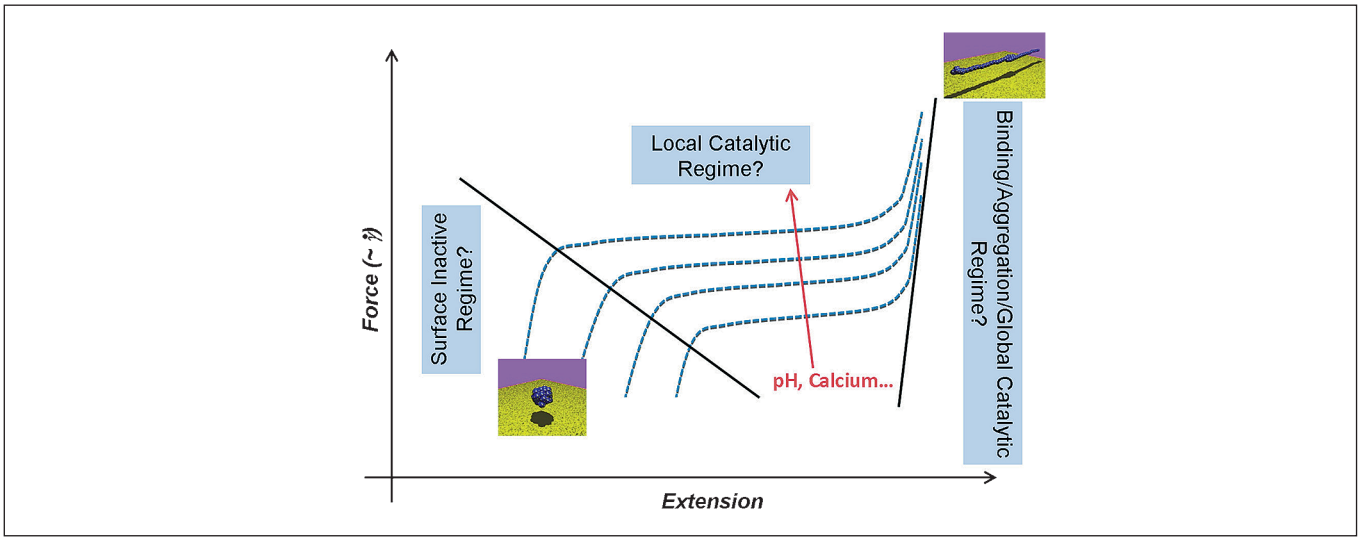

Figure 4: Hypothetical state-function relationship of VWF. The force-extension curve and hence the globule-stretched transition $\dot{\gamma}_{crit}$ varies with pH, calcium and other ions, temperature, binding of albumin etc. (red arrow) resulting in a dynamic state-diagram of VWF. A certain physical state is proposed to be associated with a certain physiological function. At high extension and force for instance VWF is rendered adhesive, while the opposite (small extension and force) creates a rather inactive state. The diagram therefore represents the state-function relationship of VWF. Within certain parts of the diagram (i.e. near transitions), state changes can take place rather abruptly and appear therefore like a "switch" between two functional regimes. Importantly, although the transition regime is proposed to demonstrate maximal catalytic activity, the activity is expected to be still significantly large in the binding regime and – to a much lesser degree – also present in the inactive state.

The state-function or thermodynamic perspective

It is important to realise, that VWF is *not only* but *also* responding to mechanical stress. Even though we so far limited our discussion to only hydrodynamic (mechanical) aspects of VWF, as this is the best explored control of VWF activation, mechanical aspects are of course only one important factor. We already mentioned that VWF is exposed to an increase in pH upon release from the WPBs. Degree of protonation will inevitably alter surface charge along the biopolymer and hence cohesive forces. Since the balance between cohesive and hydrodynamic forces determines the critical shear rate (22), pH variations will consequently lead to changes in critical shear, which is experimentally confirmed by the work of several authors (53, 70) and preliminary data of our group. In this context it was recently shown that VWF keeps attached in a globular conformation on EC surface upon acidic conditions (pH 6.5) but gets elongated and released upon realkalinisation (51). A hypothetical experiment in which one holds the shear rate fixed and varies the pH until the transition takes place therefore demonstrates the misleading character of terms like "mechanical" or "pH-activated" molecules. Such a terminology refers rather to the experimental conditions than the physical nature of the transition. Similar results are expected for calcium and temperature changes. Indeed, we expect variations in $\dot{\gamma}_{crit}$ when any physical, chemical or biological quantity is altered: Changing ion concentrations, binding of other proteins present in blood (e.g. albumin, factor VIII), variation in degree of glycosylation, presence of cell surfaces or last but not least mutations in VWF directly. We recently could show that N-deglycosylation decreases the critical shear rate to activate soluble VWF (71). We conclude, that the proper description should be adapted from thermodynamics, where the dependence of transitions (here $\dot{\gamma}_{crit}$ - or force-variable curves (e.g $\dot{\gamma}$ - extension) - on external parameters (e.g. temperature, pH, ion-strength or protein concentration) are represented by so-called state-diagrams. Here, we propose to assign different functions or functional regimes to distinct states and therefore we suggest for diagrams like ▶Figure 4 the term *state-function diagram*. For instance, as already demonstrated, under increased shear rate and hence increased hydrodynamic force, the protein "switches" into its adhesive or binding-active state. The state below the transition may be – at least presently – called the inactive regime. We currently investigate the role of the transition state itself and propose that it is within this regime, where catalytic activity – granted full accessibility of the cleavage site – is maximised, but this has yet to be confirmed experimentally. We believe that this more general, thermodynamic approach is superior over the more classical mechano-functional or mechano-enzymatic view and describes the various physical, chemical and biological aspects that modify protein function more properly.

Methodological developments for experimental *in vitro* characterisation

The methodological *in vitro* setting to investigate the characteristics of VWF physiology has certain requirements: a planar microfluidic channel system providing for the application of a wide-ranged shear regimen combined with microscopic equipment for live-imaging with high temporal and spatial resolution is a prerequisite to cope with the free floating or anchorage-point immobilised polymer under dynamic conditions. These requirements are excellently met by combining modern microfluidic tools with label-free reflectance interference contrast microscopy (RICM) as already published (72-74). Briefly, the interference of the polarised object beam and the reference beams results in a

Table 1: Comparative summary of VWF states. For selected shear rates at distinct VWF states (see Figure 6), we summarise recent characterisations of shear-dependent VWF-VWF and VWF-platelet interactions.

$\dot{\gamma}_{crit} \sim \frac{1}{a^3}$ reflects the critical shear rate of the indicated state transition of VWF; F_{trans} reflects the necessary force for bond state transition.

Shear rate $\dot{\gamma}$ [s^{-1}]	~50	~2,000	~5,000	Ref.
VWF (EC-anchored) $\dot{\gamma}_{crit} \approx 200\ s^{-1}$	globular	stretched	stretched	(60)
VWF (soluble) $\dot{\gamma}_{crit} \approx 2{,}000\ s^{-1}$	globular	gobular → stretched	stretched	(23)
VWF-colloid interactions $\dot{\gamma}_{crit} \approx 4{,}000\ s^{-1}$	single platelet rolling	platelet decorated VWF fibres	rolling aggregates	(72)
VWF-GPIba (catch-slip bond) $F_{trans} \approx 20$ pN [a]	catch bond [b]	catch bond → slip bond [b]	slip bond [b]	(37, 78)
VWF-GPIba (flex bond) $F_{trans} \approx 10$ pN [c]	state 1 – short lifetime [d]	state 1 – short lifetime [d]	state 2 – long lifetime [e]	(69)

[a] based on atomic force microscopy experiments; [b] classification based on fluidic experiments using surface immobilised VWF; [c] based on optical tweezer experiments; [d] assumed classification by the authors; [e] classification based on the assumed tensile force acting on a soluble VWF 200-mer.

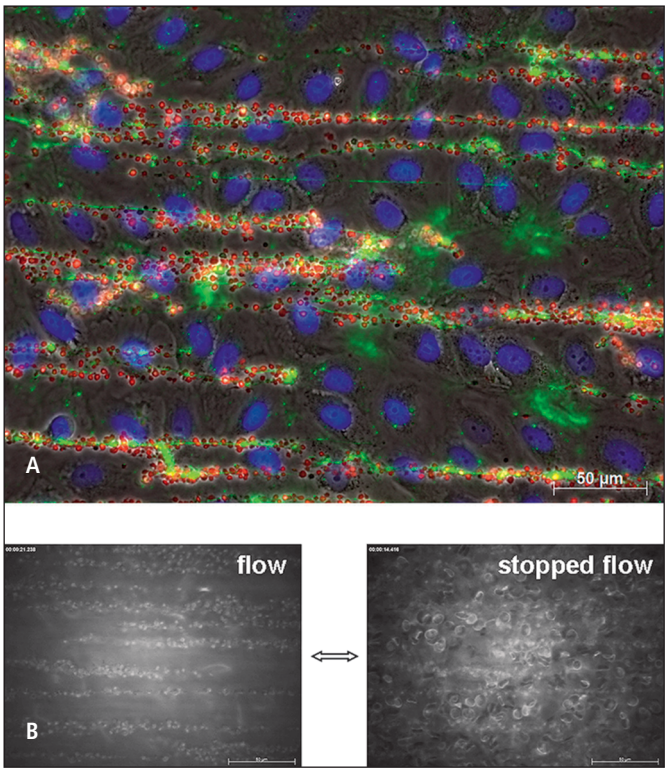

Figure 5: VWF-platelet interaction on stimulated ECs under whole blood flow conditions. A) An intact human EC layer (nuclei are stained in blue), seeded in a planar microfluidic system, is stimulated and perfused with whole blood. EC-released and still anchored VWF fibres (green) are stretched to several hundred micrometers under flow conditions and efficiently bind platelets (red). B) RICM images of stimulated ECs perfused with whole blood. Platelet decorated VWF fibres are completely stretched upon a shear rate of 2,000 s^{-1} and reversibly recoil when stopping the flow (see also Suppl. Movie 1, available online at www.thrombosis-online.com). Scale bars correspond to 50 µm.

height profile image of the observed objects at the footprint of the microfluidic channel in high resolution. Thereby, RICM facilitates both the investigation of recombinant wild-type or mutant VWF and a native functional analysis of blood samples.

For further high-value visualisation techniques with the advantage of nanometer-scaled resolution one has to dispense with live-imaging in utilising electron microscopy (75) or atomic force microscopy, the latter with the further potential of force spectroscopic measurements (76, 77). But for these microscopic techniques, we agree with Ruggeri's anniversary issue contribution from 2007: It has to be taken into consideration that for the necessary fixation of the observed molecules one has to focus on the immobilised fraction of VWF and therefore there is no proof for an exact assignability of VWF's functional characteristics (33).

Dynamics of VWF-colloid interactions

Notwithstanding, at the site of inflamed endothelium and the downstream vasculature there are both EC-anchored VWF multimers and a plenty of soluble VWF fibre fragments, capable for re-polymerisation, for direct surface or for colloid interactions also on an intact endothelial layer (13, 14, 59). As shown in ▶Figure 5A, above the critical shear rate of about 200 s^{-1} (19, 60) these EC-anchored fibres recruit platelets under whole blood conditions resulting in complete platelet decorated strings. This experiment was performed in an *in vitro* microfluidic channel system in the absence of ADAMTS13. For illustration of the dynamic elongational force of shear flow, images from a life-cell movie (see Suppl. Movie 1, available online at www.thrombosis-online.com) are presented in ▶Figure 5B upon a shear rate of 2,000 s^{-1} (complete stretched fibres) and short-termed stopped flow (recoiling fibres).

Next to the shear-dependent consideration of VWF multimers, also the particular binding between GPIba and VWF A1 domain has been extensively studied by several groups. To characterise the acting biophysical mechanisms, catch-slip (37, 78) or flex (79) bonds have been proposed. What type of bond stabilises and/or controls VWF interaction with platelets or the vessel wall is therefore matter of recent discussion. The authors do not believe that there is consensus and are not aware of any thorough experimental studies considering the role of e.g. the membrane state or the hydration layer for bonds association. A comparative summary of recently proposed classifications regarding shear dependencies of VWF-VWF and VWF-platelet interactions is given in ▶Table 1. For further specifications we like to refer the reader to the work of other authors (37, 39, 53, 78, 79).

It was recently shown *in vitro* that under whole blood conditions only by application of high-shear the soluble fraction of VWF interacts with platelets (in general: colloids) above a critical aggregation shear rate of ~4,000 s^{-1} (see ▶Table 1). Polymer-colloid composites (rolling aggregates) with a total three-dimensional circumference of up to 200 µm are generated, rolling on a VWF biofunctionalised surface. To be clear, rolling aggregates represent the self-assembly of VWF multimers binding platelets to form conglomerates of a few hundred micrometers in size. When lowering the shear flow, these composites are reversible, fully dissolving below the aggregation shear rate (72). Interestingly, the occurrence and dissolving is initially independent of the presence of ADAMTS13. However, one has to keep in mind that all theses experiments were done in the presence of an artificial platelet inhibition (33, 73, 80). Furthermore, colloid binding to the shear-induced exposed A1 domain seems to be one of the key factors for the process of rolling aggregate formation as GPIba-coated silicate beads are also capable to induce aggregation (72). These reversible transitions from globular to stretched to aggregation conformations including colloid interactions are depicted in ▶Figure 6.

Recent insights into the impact of VWF

These rolling aggregates envision a new insight into VWF characteristics at high shear rates. Although the pathophysiological impact is not yet understood, it is clearly shown that polymer-colloid composites require the presence of free soluble VWF. This process

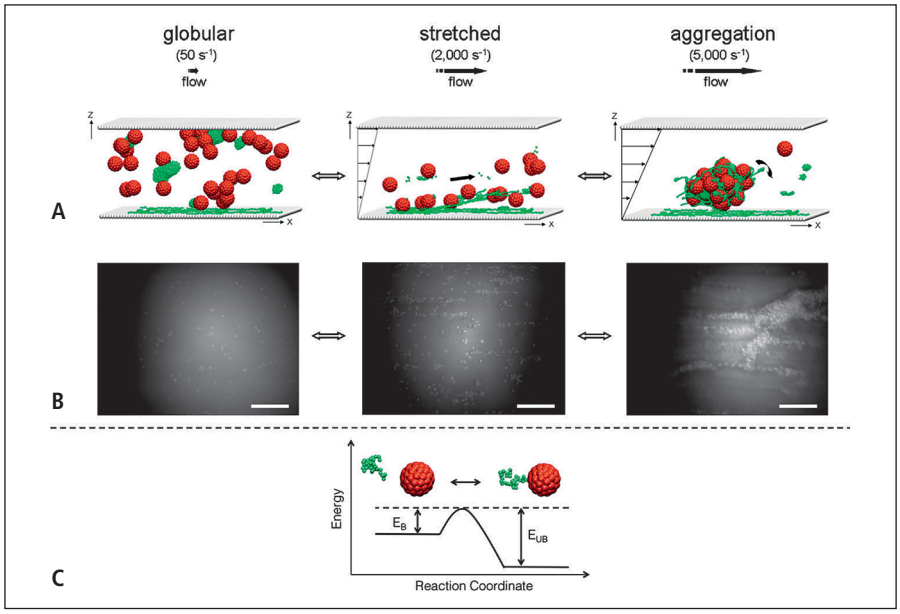

Figure 6: VWF-colloid interactions from globular to stretched to aggregation transition. (Figure based on our earlier work (72), doi:10.1038/ncomms2326, Fig. 1). Schematics of simulation snapshots (A) and RICM movie snapshots (B) of human whole blood supplemented with soluble VWF on a VWF biofunctionalised surface. At low-flow conditions only single platelets (colloids, red in A, white dots in B) interact with the surface (left). Above a critical$_{fibre}$ shear rate, VWF (green) recruited from the bulk reversibly build fibre-like structures and bind colloids (middle). Under high-shear conditions (with a critical$_{aggregate}$ shear rate of ~4,000 s^{-1}) reversible VWF-colloid aggregates appear rolling on the surface, dissolving after reducing the shear rate. Scale bars correspond to 50 µm. C) The energy landscape for a single associating pair of one monomer and one colloid binding site. The energy to form this bond is given by E_B, and the barrier to break this bond is given by E_{UB}.

is most likely VWF A1 domain-GPIba dependent, as an inhibition of GPIba leads to a complete abolishment of both single rolling platelets on the immobilised VWF surface and aggregation (72). One can speculate that this process is mainly required in a situation of extremely high shear rates as present in stenotic vessels. This VWF-platelet aggregate formation may therefore be the reason for the complete occlusion of such a vessel, in line with animal experiments demonstrating that thrombus formation does not require VWF; however, the final vessel occlusion in veins (81) and arteries (82, 83). Further strengthening the fluid dynamic part in VWF elongation and VWF-interactions with its binding partners, McKinnon et al. prove a higher affinity of ADAMTS13 to VWF after specific deglycosylation of VWF N-glycans (84). In concordance, also an enhanced binding of platelets to VWF after complete N-deglycosylation is stated (71).

Regarding the role of VWF in inflammatory processes recent *in vitro* studies suggest a direct binding of leukocytes to VWF via P-selectin glycoprotein ligand-1 and beta2-integrins thereby further facilitating leukocyte extravasation (85, 86). In ADAMTS13 knockout mice ULVWF is mainly involved in leukocyte extravasation and may be involved in enhanced WPB exocytosis in an autocrine manner (61). Furthermore, in a murine peritonitis and vasculitis model endothelial-derived VWF plays a pivotal role for leukocyte extravasation (87, 88). Finally, Pappelbaum et al. demonstrate that S*taphylococcus aureus* bind to VWF strings but not to non-elongated VWF multimers under *in vitro* flow conditions on activated endothelium whereas the VWF-independent binding to other endothelial exposed molecules remains negligible (►Figure 7) (60), confirmed in a VWF knockout mouse model. The presented results may explain the mechanism of *S. aureus* infection of heart valves in the absence of an injured or damaged vascular system. Therefore, VWF is also considerable as an inflammatory molecule bridging coagulation and inflammation in vari-

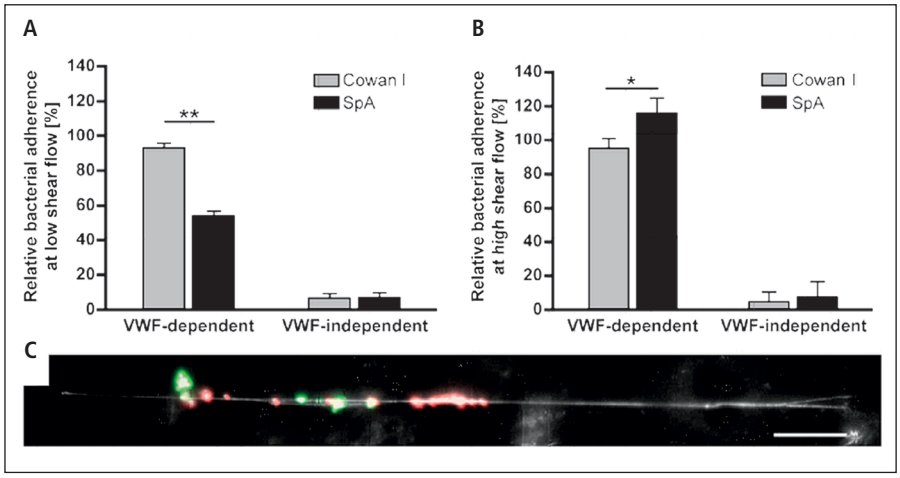

Figure 7: *Staphylococcus aureus* binding to VWF. (Figure of our earlier work (60), doi:10.1161/CIRCULATIONAHA.113.002008, Fig. 4). A) Under low-shear flow conditions, adhesion of *S. aureus* SpA was decreased compared with *S. aureus* Cowan I. B) Under high-shear flow conditions, adhesion of *S. aureus* SpA was increased (n=5). *S. aureus* Cowan I adhesion was normalised to 100%, and adhesion of *S. aureus* SpA is represented relative to *S. aureus* Cowan I adhesion. Data are expressed as mean + SD (* $p < 0.05$, ** $p < 0.001$). C) Representative fluorescence image of *S. aureus* Cowan I (green) and *S. aureus* SpA (red) bound to an ultra-large VWF (ULVWF) fibre (white) under high-shear flow conditions. Scale bar corresponds to 20 µm.

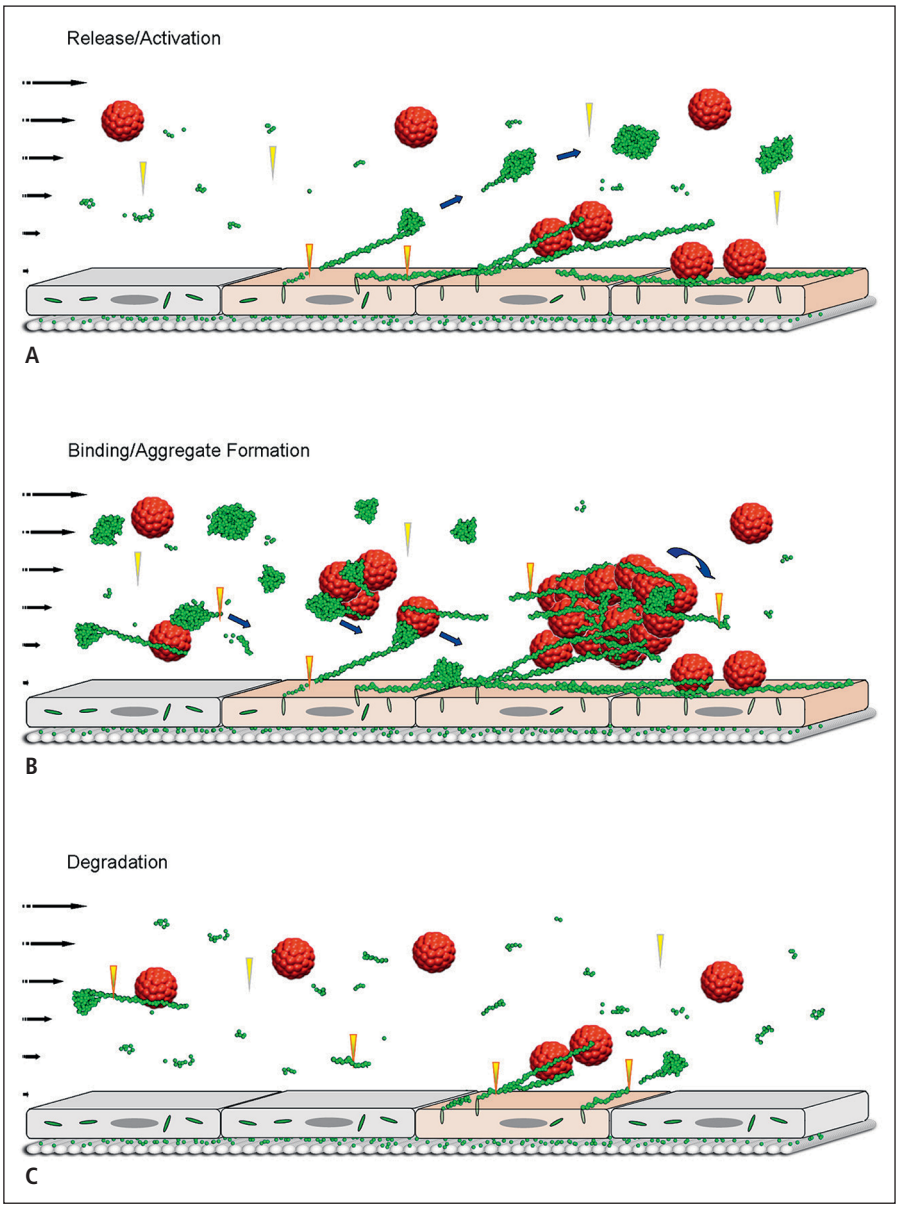

Figure 8: Three steps in lifecycle of VWF in human vasculature. A) Release/Activation: Upon EC stimulation (orange highlighted ECs), long VWF multimers (green) are released by WPBs. Exposed to the blood flow VWF fibres, still locally anchored at the endothelial surface, are stretched and interact with surrounding colloids (red). Cleaved from the endothelium by ADAMTS13 (yellow triangles), these multimeric VWF fibres recoil (blue arrows) and are transported to the downstream vasculature. B) Binding/Aggregate Formation: These soluble high molecular weight VWF multimers, shielded from further degradation, become immediately reactivated e.g. at the site of inflamed endothelium. In a short time frame, soluble VWF is recruited (blue arrows) for intensified colloid binding or VWF-colloid aggregation. C) Degradation: VWF becomes functionally inactivated by further processes of degradation. Re-polymerisation of the small oligomers is still feasible, but now tightly controlled by physiological VWF-ADAMTS13 interactions.

ous forms and shapes as recently also described by Rauch et al. (89).

The lifecycle of VWF in human vasculature

Taking together these established results and the presented new insights, we might reconstruct VWF biology and its characteristic interactions from endothelial release to final functional degradation in the human vasculature. Next to deposition into the subendothelial matrix and its isolated well-studied role upon vessel injury (3-6, 9, 28, 47), the main focus is put on the intraluminal VWF and its impact on both haemostatic and inflammatory processes. As schematically depicted in ▶Figure 8, we suggest three steps in the lifecycle of VWF, all of them mainly influenced by the predominant local shear flow and the composition of the surrounding microenvironment (e.g. local pH, ion concentrations, temperature etc.):

The first step (▶Figure 8A, "Release") is the stimulated release of long VWF multimers by endothelial WPB still locally anchored at the EC surface. Exposed to the blood flow, these anchor-point immobilised polymers become easily stretched and can rapidly interact with surrounding colloids (i.e. blood components as platelets, leukocytes or pathogens/bacteria). The shear-induced activation of VWF is strongly influenced by the local microenvironment. But concomitantly, the binding affinity to as well as the activity of ADAMTS13 is affected and will determine the time frame of VWF's action and degradation.

The subsequent dissociation from the endothelium, mainly induced by the first cleavage by ADAMTS13, leads to the second

step in the life of VWF (►Figure 8B, "Binding/Aggregate formation"). The freshly cleaved VWF multimers of still high molecular weight will recoil due to the shift of the critical transition shear rate for the now free floating polymer and are, shielded from further degradation by ADAMTS13, transported to the downstream vasculature. However, their capability for an immediate reactivation and therefore a re-polymerisation at the site of inflamed endothelium (90), vessel injuries or pathological high shear areas in the downstream is still present. High local concentrations of this soluble VWF immediately initiate colloid binding (stretched transition) or VWF-colloid aggregation (aggregation transition). Subsequent time-dependent degradation by ADAMTS13 upon its next activation leads to the third step in the life of VWF (►Figure 8C, "Degradation").

By multiple degradation processes, soluble VWF becomes functionally inactive and is finally cleared in the liver and spleen (91). Due to the dynamic equilibrium of physiological VWF-ADAMTS13 interactions, here the ability to form long fibres is diminished or completely abolished.

Conclusion

Despite recent advancements in the understanding of VWF as a shear stress sensitive protein, the role of its domains during binding and degradation, we would like to point out several open areas, which remain largely unexplored. First, there is a clear discrepancy between the size of VWF multimers as seen in classical gel electrophoresis (indicating a size of up to ~50 MDa) and the size of VWF fibres observed under high shear flow conditions *in vitro*, which are approx. 100 times larger. Importantly, only the latter ones are consistent with the size of VWF stored in individual WPBs (~1 GDa). Second, collective phenomena can result in even larger assemblies either between VWF with itself or between VWF and additional blood components (72). So far, the physiological role of VWF biopolymers in the size range of GDa as well as the even larger aggregates, although experimentally identified, remains entirely unclear mainly due to methodological limitations. Finally, we would like to emphasise, that despite the obvious role of VWF's size, further factors will regulate its state and hence its activation and degradation under flow. Such factors may be imagined as pH (51), degree of oxidation (92), glycosylation (71, 84), binding of other molecules and mutations. We propose, that only such an universal approach will probably be able to lead to a deeper understanding of VWF related diseases and may explain the various facets of TTP and VWD-related clinical manifestations.

Acknowledgements

The authors acknowledge kind support from the German Research Foundation (DFG) SHENC - Research Unit FOR1543, project VH/SWS A2, MFS for a guest professorship and SFB/Transregio 23, project SWS A9. The authors thank Prof. R. Schneppenheim (University Medical Centre Hamburg-Eppendorf, Germany) and Prof. U. Budde (AescuLabor, Hamburg, Germany) for valuable suggestions and fruitful scientific discussions. Moreover, the authors thank Prof. A. Alexander-Katz (MIT, Cambridge, USA), Dr. D. Steppich (University of Augsburg, Germany) and Dr. S. Bössinger (Boston University, USA) for their contributions and B. Schneider for design of artwork.

Conflicts of interest

None declared.

References

1. Cheng H, Yan R, Li S, et al. Shear-induced interaction of platelets with von Willebrand factor results in glycoprotein Ibalpha shedding. Am J Physiol Heart Circ Physiol 2009; 297: H2128-2135.
2. Hanson E, Jood K, Karlsson S, et al. Plasma levels of von Willebrand factor in the etiologic subtypes of ischemic stroke. J Thromb Haemost 2011; 9: 275-281.
3. Mannucci PM. von Willebrand factor: a marker of endothelial damage? Arterioscler Thromb Vasc Biol 1998; 18: 1359-1362.
4. Mendolicchio GL, Ruggeri ZM. New perspectives on von Willebrand factor functions in hemostasis and thrombosis. Semin Hematol 2005; 42: 5-14.
5. Moroose R, Hoyer LW. von Willebrand factor and platelet function. Annu Rev Med 1986; 37: 157-163.
6. Ruggeri ZM. Structure of von Willebrand factor and its function in platelet adhesion and thrombus formation. Best Pract Res Clin Haematol 2001; 14: 257-279.
7. Ruggeri ZM. The role of von Willebrand factor in thrombus formation. Thromb Res 2007; 120 (Suppl 1): S5-9.
8. Ruggeri ZM, Orje JN, Habermann R, et al. Activation-independent platelet adhesion and aggregation under elevated shear stress. Blood 2006; 108: 1903-1910.
9. Sadler JE. Biochemistry and genetics of von Willebrand factor. Annu Rev Biochem 1998; 67: 395-424.
10. Huck V, Niemeyer A, Goerge T, et al. Delay of acute intracellular pH recovery after acidosis decreases endothelial cell activation. J Cell Physiol 2007; 211: 399-409.
11. Wagner DD, Frenette PS. The vessel wall and its interactions. Blood 2008; 111: 5271-5281.
12. Desch A, Strozyk EA, Bauer AT, et al. Highly Invasive Melanoma Cells Activate the Vascular Endothelium via an MMP-2/Integrin αvβ5–Induced Secretion of VEGF-A. Am J Pathol 2012; 181: 693-705.
13. Fallah MA, Myles VM, Kruger T, et al. Acoustic driven flow and lattice Boltzmann simulations to study cell adhesion in biofunctionalized mu-fluidic channels with complex geometry. Biomicrofluidics 2010; 4: 024106 1-10.
14. Goerge T, Kleineruschkamp F, Barg A, et al. Microfluidic reveals generation of platelet-strings on tumor-activated endothelium. Thromb Haemost 2007; 98: 283-286.
15. Kerk N, Strozyk EA, Poppelmann B, et al. The mechanism of melanoma-associated thrombin activity and von Willebrand factor release from endothelial cells. J Invest Dermatol 2010; 130: 2259-2268.
16. Schneider SW, Larmer J, Henderson RM, et al. Molecular weights of individual proteins correlate with molecular volumes measured by atomic force microscopy. Pflugers Arch Eur J Physiol 1998; 435: 362-367.
17. Furlan M. Von Willebrand factor: molecular size and functional activity. Ann Hematol 1996; 72: 341-348.
18. Schneppenheim R, Lenk H, Obser T, et al. Recombinant expression of mutations causing von Willebrand disease type Normandy: characterization of a combined defect of factor VIII binding and multimerization. Thromb Haemost 2004; 92: 36-41.
19. Dong JF, Moake JL, Nolasco L, et al. ADAMTS-13 rapidly cleaves newly secreted ultralarge von Willebrand factor multimers on the endothelial surface under flowing conditions. Blood 2002; 100: 4033-4039.
20. Metcalf DJ, Nightingale TD, Zenner HL, et al. Formation and function of Weibel-Palade bodies. J Cell Sci 2008; 121: 19-27.
21. Barg A, Ossig R, Goerge T, et al. Soluble plasma-derived von Willebrand factor assembles to a haemostatically active filamentous network. Thromb Haemost 2007; 97: 514-526.

22. Alexander-Katz A, Schneider MF, Schneider SW, et al. Shear-flow-induced unfolding of polymeric globules. Physical Rev Lett 2006; 97: 138101.
23. Schneider SW, Nuschele S, Wixforth A, et al. Shear-induced unfolding triggers adhesion of von Willebrand factor fibers. Proc Natl Acad Sci 2007; 104: 7899-7903.
24. Goerge T, Barg A, Schnaeker EM, et al. Tumor-derived matrix metalloproteinase-1 targets endothelial proteinase-activated receptor 1 promoting endothelial cell activation. Cancer Res 2006; 66: 7766-7774.
25. Goerge T, Niemeyer A, Rogge P, et al. Secretion pores in human endothelial cells during acute hypoxia. J Membr Biol 2002; 187: 203-211.
26. Terraube V, Marx I, Denis CV. Role of von Willebrand factor in tumor metastasis. Thromb Res 2007; 120 (Suppl 2): S64-70.
27. Haberichter SL, Fahs SA, Montgomery RR. von Willebrand factor storage and multimerization: 2 independent intracellular processes. Blood 2000; 96: 1808-1815.
28. Wagner DD. Cell biology of von Willebrand factor. Annu Rev Cell Biol 1990; 6: 217-246.
29. Singh I, Themistou E, Porcar L, et al. Fluid shear induces conformation change in human blood protein von Willebrand factor in solution. Biophys J 2009; 96: 2313-2320.
30. Wijeratne SS, Botello E, Yeh HC, et al. Mechanical activation of a multimeric adhesive protein through domain conformational change. Phys Rev Lett 2013; 110: 108102.
31. Doggett TA, Girdhar G, Lawshe A, et al. Selectin-like kinetics and biomechanics promote rapid platelet adhesion in flow: the GPIb(alpha)-vWF tether bond. Biophys J 2002; 83: 194-205.
32. Savage B, Saldivar E, Ruggeri ZM. Initiation of platelet adhesion by arrest onto fibrinogen or translocation on von Willebrand factor. Cell 1996; 84: 289-297.
33. Ruggeri ZM. Von Willebrand factor: looking back and looking forward. Thromb Haemost 2007; 98: 55-62.
34. Konstantinides S, Ware J, Marchese P, et al. Distinct antithrombotic consequences of platelet glycoprotein Ibalpha and VI deficiency in a mouse model of arterial thrombosis. J Thromb Haemost 2006; 4: 2014-2021.
35. Savage B, Almus-Jacobs F, Ruggeri ZM. Specific synergy of multiple substrate-receptor interactions in platelet thrombus formation under flow. Cell 1998; 94: 657-666.
36. Nesbitt WS, Westein E, Tovar-Lopez FJ, et al. A shear gradient-dependent platelet aggregation mechanism drives thrombus formation. Nat Med 2009; 15: 665-673.
37. Yago T, Lou J, Wu T, et al. Platelet glycoprotein Ibalpha forms catch bonds with human WT vWF but not with type 2B von Willebrand disease vWF. J Clin Invest 2008; 118: 3195-3207.
38. Colace TV, Diamond SL. Direct observation of von Willebrand factor elongation and fiber formation on collagen during acute whole blood exposure to pathological flow. Arterioscler Thromb Vasc Biol 2013; 33: 105-113.
39. Sing CE, Selvidge JG, Alexander-Katz A. Von Willlebrand adhesion to surfaces at high shear rates is controlled by long-lived bonds. Biophys J 2013; 105: 1475-1481.
40. Levy GG, Nichols WC, Lian EC, et al. Mutations in a member of the ADAMTS gene family cause thrombotic thrombocytopenic purpura. Nature 2001; 413: 488-494.
41. Schneppenheim R, Budde U. von Willebrand factor: the complex molecular genetics of a multidomain and multifunctional protein. J Thromb Haemost 2011; 9: 209-215.
42. Kasatkar P, Ghosh K, Shetty S. An atypical manifestation of acquired von Willebrand syndrome (AVWS) associated with systemic lupus erythematosus (SLE). Ann Hematol 2013; 93: 173-175.
43. Vincentelli A, Susen S, Le Tourneau T, et al. Acquired von Willebrand syndrome in aortic stenosis. N Engl J Med 2003; 349: 343-349.
44. Tiede A, Priesack J, Werwitzke S, et al. Diagnostic workup of patients with acquired von Willebrand syndrome: a retrospective single-centre cohort study. J Thromb Haemost 2008; 6: 569-576.
45. Moake JL. von Willebrand factor, ADAMTS-13, and thrombotic thrombocytopenic purpura. Semin Hematol 2004; 41: 4-14.
46. Moake JL, Rudy CK, Troll JH, et al. Unusually large plasma factor VIII:von Willebrand factor multimers in chronic relapsing thrombotic thrombocytopenic purpura. N Engl J Med 1982; 307: 1432-1435.
47. Moake JL. The role of von Willebrand factor (vWF) in thrombotic thrombocytopenic purpura (TTP) and the hemolytic-uremic syndrome (HUS). Prog Clin Biol Res 1990; 337: 135-140.
48. Bernardo A, Ball C, Nolasco L, et al. Effects of inflammatory cytokines on the release and cleavage of the endothelial cell-derived ultralarge von Willebrand factor multimers under flow. Blood 2004; 104: 100-106.
49. Chen J, Fu X, Wang Y, et al. Oxidative modification of von Willebrand factor by neutrophil oxidants inhibits its cleavage by ADAMTS13. Blood 2009; 115: 706-712.
50. Crawley JT, Lane DA, Woodward M, et al. Evidence that high von Willebrand factor and low ADAMTS-13 levels independently increase the risk of a non-fatal heart attack. J Thromb Haemost 2008; 6: 583-588.
51. Babich V, Knipe L, Hewlett L, et al. Differential effect of extracellular acidosis on the release and dispersal of soluble and membrane proteins secreted from the Weibel-Palade body. J Biol Chem 2009; 284: 12459-12468.
52. Erent M, Meli A, Moisoi N, et al. Rate, extent and concentration dependence of histamine-evoked Weibel-Palade body exocytosis determined from individual fusion events in human endothelial cells. J Physiol 2007; 583: 195-212.
53. Springer TA. Biology and physics of von Willebrand factor concatamers. J Thromb Haemost 2011; 9 (Suppl 1): 130-143.
54. Babich V, Meli A, Knipe L, et al. Selective release of molecules from Weibel-Palade bodies during a lingering kiss. Blood 2008; 111: 5282-5290.
55. Berriman JA, Li S, Hewlett LJ, et al. Structural organization of Weibel-Palade bodies revealed by cryo-EM of vitrified endothelial cells. Proc Natl Acad Sci USA 2009; 106: 17407-17412.
56. Huang J, Roth R, Heuser JE, et al. Integrin alpha(v)beta(3) on human endothelial cells binds von Willebrand factor strings under fluid shear stress. Blood 2009; 113: 1589-1597.
57. Padilla A, Moake JL, Bernardo A, et al. P-selectin anchors newly released ultralarge von Willebrand factor multimers to the endothelial cell surface. Blood 2004; 103: 2150-2156.
58. Roberts DD, Williams SB, Gralnick HR, et al. von Willebrand factor binds specifically to sulfated glycolipids. J Biol Chem 1986; 261: 3306-3309.
59. Chauhan AK, Goerge T, Schneider SW, et al. Formation of platelet strings and microthrombi in the presence of ADAMTS-13 inhibitor does not require P-selectin or beta3 integrin. J Thromb Haemost 2007; 5: 583-589.
60. Pappelbaum KI, Gorzelanny C, Grassle S, et al. Ultralarge von Willebrand Factor Fibers Mediate Luminal Staphylococcus aureus Adhesion to an Intact Endothelial Cell Layer Under Shear Stress. Circulation 2013; 128: 50-59.
61. Chauhan AK, Kisucka J, Brill A, et al. ADAMTS13: a new link between thrombosis and inflammation. J Exp Med 2008; 205: 2065-2074.
62. Brill A, Fuchs TA, Chauhan AK, et al. von Willebrand factor-mediated platelet adhesion is critical for deep vein thrombosis in mouse models. Blood 2011; 117: 1400-1407.
63. Tangelder GJ, Slaaf DW, Arts T, et al. Wall shear rate in arterioles in vivo: least estimates from platelet velocity profiles. Am J Physiol 1988; 254: H1059-1064.
64. Truskey GA, Yuan F, Katz DF. Transport Phenomena in Biological Systems. 2nd ed. Prentice Hall, Upper Saddle River, New Jersey 07458; 2009.
65. Back LD, Radbill JR, Crawford DW. Analysis of pulsatile, viscous blood flow through diseased coronary arteries of man. J Biomech 1977; 10: 339-353.
66. Westein E, van der Meer AD, Kuijpers MJ, et al. Atherosclerotic geometries exacerbate pathological thrombus formation poststenosis in a von Willebrand factor-dependent manner. Proc Natl Acad Sci USA 2013; 110: 1357-1362.
67. Singh I, Shankaran H, Beauharnois ME, et al. Solution structure of human von Willebrand factor studied using small angle neutron scattering. J Biol Chem 2006; 281: 38266-38275.
68. Sing CE, Alexander-Katz A. Elongational flow induces the unfolding of von Willebrand factor at physiological flow rates. Biophys J 2010; 98: L35-37.
69. Zhang X, Halvorsen K, Zhang CZ, et al. Mechanoenzymatic cleavage of the ultralarge vascular protein von Willebrand factor. Science 2009; 324: 1330-1334.
70. Tsai HM. Physiologic cleavage of von Willebrand factor by a plasma protease is dependent on its conformation and requires calcium ion. Blood 1996; 87: 4235-4244.
71. Fallah MA, Huck V, Niemeyer V, et al. Circulating but not immobilized N-deglycosylated von Willebrand factor increases platelet adhesion under flow conditions. Biomicrofluidics 2013; 7: 044124.
72. Chen H, Fallah MA, Huck V, et al. Blood-clotting-inspired reversible polymer-colloid composite assembly in flow. Nat Commun 2013; 4: 1333.

73. Reininger AJ. Platelet function under high shear conditions. Hamostaseologie 2009; 29: 21-22, 24.
74. Reininger AJ. Function of von Willebrand factor in haemostasis and thrombosis. Haemophilia 2008; 14 (Suppl 5): 11-26.
75. Zhou YF, Eng ET, Zhu J, et al. Sequence and structure relationships within von Willebrand factor. Blood 2012; 120: 449-458.
76. Friedrichs J, Legate KR, Schubert R, et al. A practical guide to quantify cell adhesion using single-cell force spectroscopy. Methods 2013; 60: 169-178.
77. Leitner M, Fantner GE, Fantner EJ, et al. Increased imaging speed and force sensitivity for bio-applications with small cantilevers using a conventional AFM setup. Micron 2012; 43: 1399-1407.
78. Ju L, Dong JF, Cruz MA, et al. The N-terminal flanking region of the A1 domain regulates the force-dependent binding of von Willebrand factor to platelet glycoprotein Ibalpha. J Biol Chem 2013; 288: 32289-32301.
79. Kim J, Zhang CZ, Zhang X, et al. A mechanically stabilized receptor-ligand flex-bond important in the vasculature. Nature 2010; 466: 992-995.
80. Reininger AJ. VWF attributes--impact on thrombus formation. Thromb Res 2008; 122 (Suppl 4): S9-13.
81. Chauhan AK, Kisucka J, Lamb CB, et al. von Willebrand factor and factor VIII are independently required to form stable occlusive thrombi in injured veins. Blood 2007; 109: 2424-2429.
82. Denis C, Methia N, Frenette PS, et al. A mouse model of severe von Willebrand disease: defects in hemostasis and thrombosis. Proc Natl Acad Sci USA 1998; 95: 9524-9529.
83. Ni H, Denis CV, Subbarao S, et al. Persistence of platelet thrombus formation in arterioles of mice lacking both von Willebrand factor and fibrinogen. J Clin Invest 2000; 106: 385-392.
84. McKinnon TA, Chion AC, Millington AJ, et al. N-linked glycosylation of VWF modulates its interaction with ADAMTS13. Blood 2008; 111: 3042-3049.
85. Weyrich AS, Lindemann S, Zimmerman GA. The evolving role of platelets in inflammation. J Thromb Haemost 2003; 1: 1897-1905.
86. Pendu R, Terraube V, Christophe OD, et al. P-selectin glycoprotein ligand 1 and beta2-integrins cooperate in the adhesion of leukocytes to von Willebrand factor. Blood 2006; 108: 3746-3752.
87. Petri B, Broermann A, Li H, et al. von Willebrand factor promotes leukocyte extravasation. Blood 2010; 116: 4712-4719.
88. Hillgruber C, Steingraber AK, Poppelmann B, et al. Blocking Von Willebrand Factor for Treatment of Cutaneous Inflammation. J Invest Dermatol 2013; 134: 77-86.
89. Rauch A, Wohner N, Christophe OD, et al. On the versatility of von Willebrand factor. Mediterr J Hematol Infect Dis 2013; 5: e2013046.
90. Yuan H, Deng N, Zhang S, et al. The unfolded von Willebrand factor response in bloodstream: the self-association perspective. J Hematol Oncol 2012; 5: 65.
91. Casari C, Lenting PJ, Wohner N, et al. Clearance of von Willebrand factor. J Thromb Haemost 2013; 11 (Suppl 1): 202-211.
92. Oggianu L, Lancellotti S, Pitocco D, et al. The oxidative modification of von Willebrand factor is associated with thrombotic angiopathies in diabetes mellitus. PLoS One 2013; 8: e55396.